Design of a Multimaterial 3D-printed Soft Actuator with Bi-directional Variable Stiffness *

Oliver Shorthose[1], Liang He[1], Alessandro Albini[1], and Perla Maiolino[1]

Oxford Robotics Institute, University of Oxford, Oxford OX1 2JD, UK
{ollies,liang,ale,perla}@robots.ox.ac.uk
https://ori.ox.ac.uk/

Abstract. A multi-material 3D printed soft actuator is presented that uses symmetrical, parallel chambers to achieve bi-directional variable stiffness. Many recent soft robotic solutions involve multi-stage fabrication, provide variable stiffness in only one direction or lack a means of reliably controlling the actuator stiffness. The use of multi-material 3D printing means complex monolithic designs can be produced without the need for further fabrication steps. We demonstrate that this allows for a high degree of repeatability between actuators and the ability to introduce different control behaviours into a single body. By independently varying the pressure in two parallel chambers, two control modes are proposed: complementary and antagonistic. We show that the actuator is able to tune its force output. The differential control significantly increases force output with controllable stiffness enabled within a safe, low-pressure range ($\leq$ 20 kPa). Experimental characterisations in angular range, repeatability between printed models, hysteresis, absolute maximum force, and beam stiffness are presented. The proposed design demonstrated a maximum bending angle of 102.6°, maximum output force 2.17N, and maximum beam stiffness 0.96mN m^2.

Keywords: Soft Robot · 3D Printing · Variable Stiffness actuator.

1 Introduction

Soft and compliant materials have been increasingly implemented into robotics research in the last decade. These soft robots have shown benefits over their rigid counterparts with regards to higher levels of safety and the ability to adapt to unknown environments or tasks [1, 2]. However, the compliance of the materials and non-linear behaviour limit precise position control and the force that can be applied to the environment [1, 3].

Various research works have proposed solutions to solve the above issues. In particular, to increase the force that can be applied, variable stiffness actuators have been proposed based on several methods [4, 5]. These solutions, based on composite materials, introduce challenges in the actuator fabrication and control

* We gratefully acknowledge support by EPSRC Programme Grant 'From Sensing to Collaboration' (EP/V000748/1)

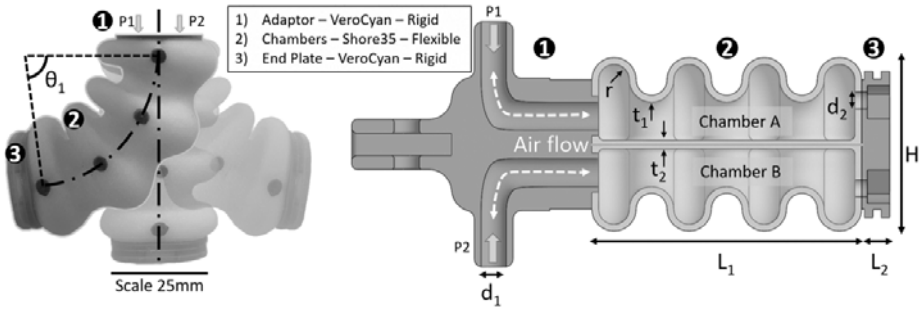

Fig. 1: Left: The multi-material actuator bent in both directions and at the neutral position. P1 and P2 are the independently applied driving pressures. θ_1 is the output angle. Right: Section view of the actuator showing the two chambers and the different regions utilising multi-material fabrication. Geometric properties are presented in mm: $r_i = 2.75$; $t_1 = 1.2$; $t_2 = 1.5$; $d_1 = 4.5$; $d_2 = 3$; $L_1 = 48$; $L_2 = 5$; $H = 31$.

because they require the integration of extra systems into the soft actuators. In contrast, antagonistic pneumatic actuators, composed of parallel chambers, achieve variable stiffness behaviour whilst avoiding the need for extra internal parts [6–8]. Many of these designs excel in one-directional bending stiffening to improve force output but are limited in having a one-sided active region [8, 9]. Bi-directional variable stiffness actuators have successfully improved the bending performance with a larger workspace [6]. However, fabricating multiple chambers in the actuator is challenging with moulding and casting methods, where multiple stages of assembly or lost-wax casting are typically needed [6, 10].

Recent advances in soft material 3D printing have provided an effective solution to quickly fabricate soft actuators precisely with high repeatability [11–13]. Compared to conventional silicone moulding methods, actuators fabricated via 3D printing can also have higher design freedom. Complex internal geometries that can optimise the bending motions can be introduced into the design [14,15]. Furthermore, recent advances in additive manufacturing have provided the ability to use multi-material printing. By introducing a variety of materials into a fully-integrated monolithic actuator, designs can be extended to exploit complex material behaviours [9, 16].

In this work, we present the design of a multi-material 3D printed soft monolithic actuator which incorporates parallel symmetrical chambers to achieve bi-directional variable stiffness. The actuator is experimentally characterised to demonstrate its performance improvements compared to the state of the art. Fig. 1 shows the printed actuator in both neutral and bent poses. The two parallel chambers can be actuated independently with two modes: complementary and antagonistic. Complementary control is the method of applying positive pressure to one chamber whilst exerting negative pressure in the other, and antagonistic control applies the same pressure in both chambers. Currently

available 3D printed soft materials are still limited in the range of elongation at break compared to conventional silicone polymers. For instance, Ecoflex 00-30 (Smooth-on [17]) has elongation at failure of 900% compared to Agilus 30 (Stratasys [18]), which exhibits a range of 220-270%. This limitation implies that 3D printed bending actuators are more prone to failure when only driven with positive pressures. To address this issue, we have proposed the two control modes, which increase the actuator workspace and force output while maintaining the capability of tunable stiffness. Crinkles are also integrated into the design to mitigate the limited material elongation where structual compliance is explored predominantly instead of material compliance.

2 Design and Fabrication of the Actuator

The actuator consists of two parallel bellow-shaped flexible chambers connected by a common midlayer. By regulating the pressure variation between the two chambers, bidirectional bending motions with tunable stiffness can be achieved. The design utilises novel 3D printing technology to maximize the ease and precision of fabrication and significantly reduces the time between design-fabrication cycles. Fig. 1 shows the schematics of the actuator with design specifications in the chambers, end plate, and base attachment.

The design consists of two expanding chambers bonded to an inextensible central layer. The compliant region expands to enforce a bending motion about the central layer with the increase of driving pressure. A bellows shape design has been incorporated to reduce the chamber's strain during expansion and facilitate easy extension/contraction of the chambers [19]. The Shore 35 Agilus/VeroCyan blend was used in the fabrication of the actuator to ensure maximum compliance. The bellow structure design further reduces the stress concentration on the material during the inflation, where a smaller principal strain is required for the material during bending. When the bellows expand, there is little tensile stress induced in the material compared to a design without bellows [13].

The parallel chambers enable variable stiffness control of the actuator without requiring the addition of granules or extra internal layers through antagonistic behaviour. Furthermore, a higher force output than a single-sided chamber (with the same driving pressure) can be achieved through complementary control behaviour. The end plate is designed to be rigid (VeroCyan) to prevent ballooning at the end which wouldn't contribute to the curvature of the body and would increase local bending strains. The surface area between the end plate and chambers was maximised to reduce warping or delamination at multi-material interfaces. Similarly to the end plate, the base is designed to be rigid to prevent unfavourable displacements when pressurised.

The relationship between bending angle, stiffness and pressure cannot simply be presented in analytical form and so optimum parameters have to be determined through simulation. A parametric analysis was run in CAD to determine the optimum geometry for the chambers. The thickness of the chamber and the inner radius of the crinkle were identified as critical parameters governing the

bending behaviour of the actuator and were applied to a grid search optimisation algorithm. The body's principal stresses and tip displacement were allocated as the key metrics. An internal pressure of 10kPa was applied to the model whilst the thickness of the material was varied between 1mm and 3mm, and the inner radius of the crinkle pattern was varied between 1.5mm and 2.75mm. These ranges were chosen to satisfy printing constraints for minimum feature size, and to ensure the overall length of the actuator was less than 50mm.The optimised design parameters are illustrated in Fig 1. The normalised simulated results of the displacement and stress were weighted towards prioritising the maximisation of the displacement over minimising the stress at a weighting ratio 5:4. The difference of the weighted values was minimised to find the optimal combination of thickness and inner radius, which was found when the chamber thickness was 1.2mm and the inner radius was 2.75mm. The overall length of the chambers is 48mm, the height is 31mm, and the weight is 35g. The central layer was empirically set to be 1.5mm.

Polyjet technology (Stratasys J735 printer) was used for multi-material printing of the actuator (VeroCyan and Agilus30). VeroCyan is a rigid plastic that has a quoted tensile strength of 50-65MPa and Shore hardness 83-86D. Agilus30 is a compliant and rubber-like material, which has a quoted tensile strength of 2.1-2.6MPa and a Shore hardness of 30A.

3 Control Setup

The actuator was controlled by an Arduino. The pneumatic setup used one Delaman air pump, four Yosoo1210 solenoid valves, and one Panasonic ADP5101 pressure sensor per chamber. The pressures were sampled at 50Hz. A 30Hz HD

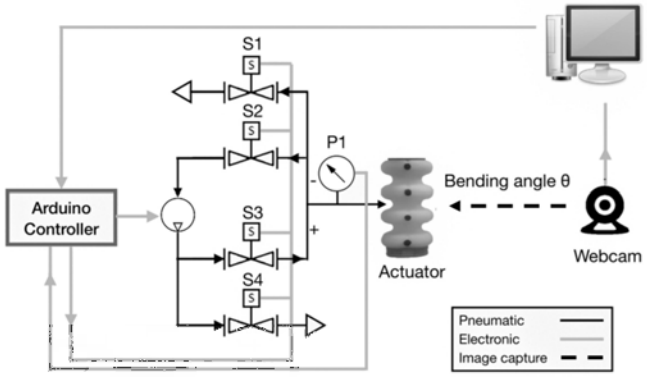

Fig. 2: Control architecture for one chamber of the soft actuator. The Arduino controls the pumps and valves, responding to real-time pressure values from the pressure sensor. The data from the Arduino and webcam is stored and post-processed to plot.

Webcam was used to acquire a video stream for angle detection. The setup is shown in Figs. 2 and 3. For the actuator characterisation, closed-loop PI (proportional-integral) control was used to compare the internal pressure value against a target value. The output of the PI control governed a pulse-width modulated (PWM) pump input, and the inflate and deflate valves. The angle of the actuator was acquired by identifying black markers down the centre of the actuator (shown in Fig. 1) and fitting them to a circular profile using a constant curvature approximation.

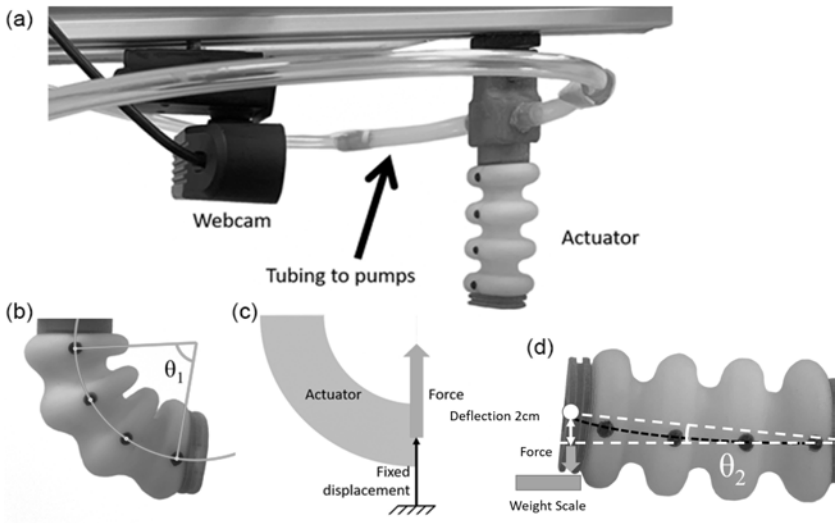

Fig. 3: (a) Experimental setup: the webcam is used for angle acquisition. (b) A circular profile is fitted to identify markers from the webcam stream to determine the angle, θ_1. (c) Complementary force test: the actuator is attached to a weight and inflated/deflated to change the force output. (d) Antagonistic stiffness test: the deflection was set at 2mm as the chambers were inflated and the force was recorded. θ_2 indicates the angle used in the small angle approximation.

4 Testing

In this section, the performance of the proposed actuator was physically tested as the bending angle versus driving pressure, hysteresis, and the effect of increased force output and tunable stiffness via complementary and antagonistic control. To evaluate differences in the printed actuators' performance, a total of 3 actuators were tested under identical experimental conditions. The actuators were tested 5 times for each test category with time between each test of more than 5 minutes to allow any residual strain energy to fully dissipate. Chambers A

and B are indicated in Fig. 1 and used interchangeably between tests to validate the bi-directionality.

Pressure versus Angle This test is used to evaluate the repeatability of the actuators' performance. Using PI control, Chamber A was inflated at a continuous rate of 0.5kPa/sec to a maximum target pressure of 16kPa with Chamber B maintained at atmospheric pressure. Although the chamber was empirically found to withstand pressures up to 22.3kPa, the targeted range was chosen to be 0-16kPa. This is to examine mid-range performance without risking breaking the actuator. Fig. 4 shows the results for a single chamber being actuated. Across all 15 tests for the 3 actuators, the single chamber actuation test shows that, at the target pressure of 16kPa, the mean angle is 44.8°, with a standard deviation of 1.3°. This translates to only a 2.9% variation compared to the full range of the test, which validates the repeatability of the fabrication method. It is also worth noting that the actuator requires lower pressures than other comparable designs [7, 9, 13].

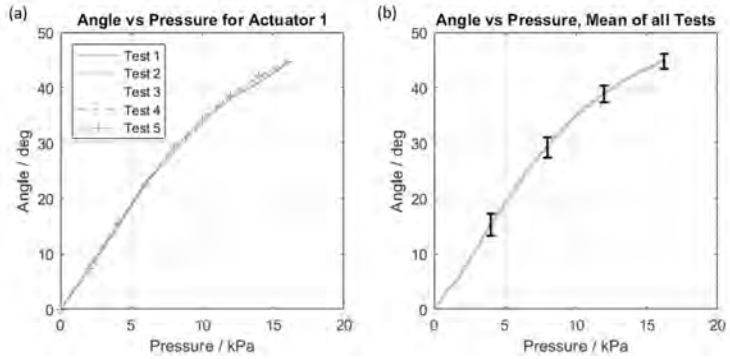

Fig. 4: Result of the single chamber pressure versus angle test. (a) 5 tests on one actuator. (b) average of 15 tests across 3 actuators.

Hysteresis The amount of hysteresis in a design can complicate the control of the system by adding a reliance on the historic behaviour of the actuator. The tests were undertaken by increasing the pressure in Chamber A by 0.5kPa/sec with PI control up to 16kPa target, holding the pressure steady for 2 seconds, and then decreasing the pressure by the same rate until the actuator returned to the neutral pose. Fig. 5 is shown with the lower curve indicating the inflation sequence and the higher curve indicating the deflation sequence. The amount of hysteresis is presented as the percentage difference between the area under the curves for the increasing and decreasing pressure cycles. This value was calculated to be 24.7%.

Complementary/Antagonistic control Using two parallel chambers, the force output and beam stiffness of the actuator can be tuned. The force output was tested for both complementary and antagonistic control.

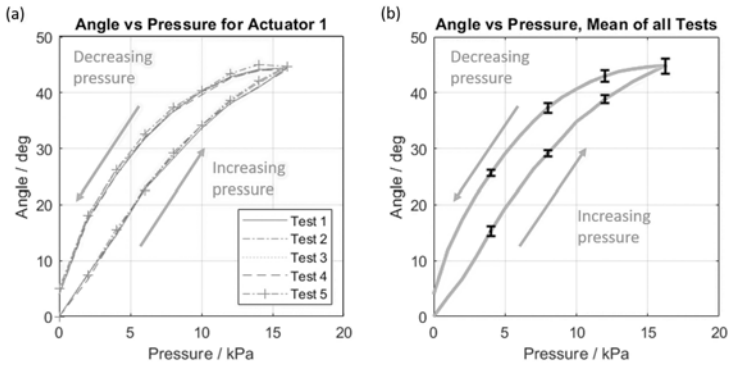

Fig. 5: Hysteresis test results. The pressure was increased/decreased at 0.5kPa/s for the inflation and deflation phases. 16kPa was the maximum targeted pressure in Chamber A before deflation. (a) 5 tests on one actuator. (b) average of 15 tests across 3 actuators.

Table 1: Complementary/Antagonistic control

		Chamber A	
		Positive Pressure	Negative Pressure
Chamber B	Positive Pressure	Antagonistic	Complementary
	Negative Pressure	Complementary	Antagonistic

The actuator's performance (Complementary control) with respect to stiffness variation was tested in terms of the actuator's maximum force. In this regard, a thread was wound around the end plate of the actuator and attached to digital weight with displacement constrained. By measuring the change in weight on a set of scales, the exerted force was deduced (Fig. 3c). For each change in pressure, the pressure was held constant for 5 seconds to ensure a static force was recorded. Chamber A was inflated to a maximum pressure of 20kPa to achieve a bent position and provide a reference force before Chamber B was depressurised to increase the force output. The depressurisation was done in 5 decrements between 0 and -22.5kPa.

The actuators' resistance to deflection (Antagonistic control) was tested by enforcing a tip deflection, pressurising the chambers, and measuring the imposed lateral force as shown in Fig. 3d. The tip was deflected by 2mm to ensure that the force being applied is normal to the end of the actuator under a small angle approximation ($\sin\theta \approx \theta$). The chambers were equally pressurised in 2kPa increments up to 20kPa with 5 seconds wait to ensure static force acquisition. Classical beam theory was applied to calculate the beam stiffness of the actuator at each pressure increment. The actuator was approximated to be a cantilever, fixed at one end, with stiffness $k = 3EI/L^3$. By applying this to Hooke's law, the beam stiffness (EI) was deduced.

To acquire a maximum force output for the actuator that can be used for benchmarking the actuator within the literature, Chamber A was pressurised to 20kPa and Chamber B was completely evacuated before the force measurement was made.

When only one chamber was actuated, the force output was 0.56N. The complementary variable force plot (Fig. 6b) shows that the design is able to increase the output force linearly by 1.56N by reducing the pressure in Chamber B. This behaviour provides an overall maximum force output of 2.17N. The antagonistic variable force plot (Fig. 6a) demonstrates that the beam stiffness of the actuator can be increased by 0.64mN m^2, which corresponds to more than a 300% increase. Whilst this is a low absolute stiffness output, it is comparable to similar work at a considerably lower pressure and validates the use of the control modes to improve the force and output of the actuator [6].

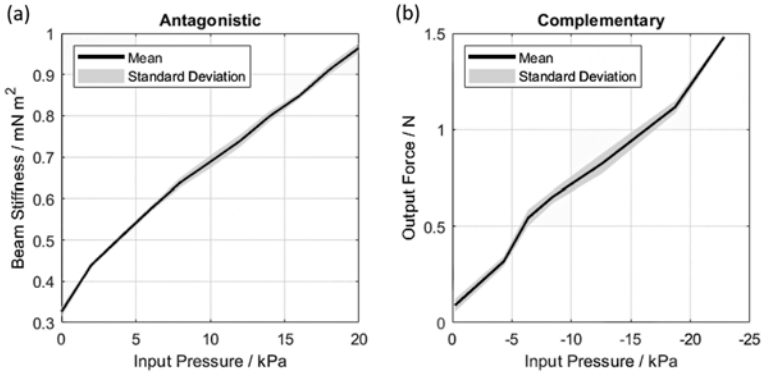

Fig. 6: (a) Result of the antagonistic actuator force test. Both chambers were inflated simultaneously from 0-20kPa in 2kPa increments. (b) Result of the complementary control force test. Chamber A was pressurised to 20kPa before starting this test and the presented data is the difference in force recorded as Chamber B was depressurised from 0 to -22.5kPa in 5kPa increments.

Effect of stiffness variation on angle The effect of independently varying the pressure in the parallel chambers leads to a change in the output angle. To enact precise position control, it is important to understand the extent of this effect for the complementary control mode. Chamber A was inflated to a single target pressure, the valves were closed, and then Chamber B was deflated. The target pressure in Chamber A was set at 13kPa and the target pressure in Chamber B was set at -10kPa. Both target pressures were, again, chosen to demonstrate the mid-range performance. The test was then used to determine a value for the maximum angle of the actuators, which can be used for easily benchmarking the design within the literature, by inflating Chamber A to 22.5kPa and deflating Chamber B to -20kPa.

The results are presented in Fig. 7 with a common x-axis to indicate the timing for the test. The test presents the effect of the change of stiffness on the actuator's angle. By actuating the second chamber, the angle is increased from 33.1° to 85.7° over the pressure change of -10kPa. This indicates that the stiffness variation has a significant effect on the output angle. This variation can be accounted for by mapping the pressure in each chamber to the output angle. The mean maximum angle across 15 samples is 85.5°, with a standard deviation of 2.9°. This corresponds to a 3.4% variation compared to the full range of the test, which further demonstrates the repeatability of the fabrication process.

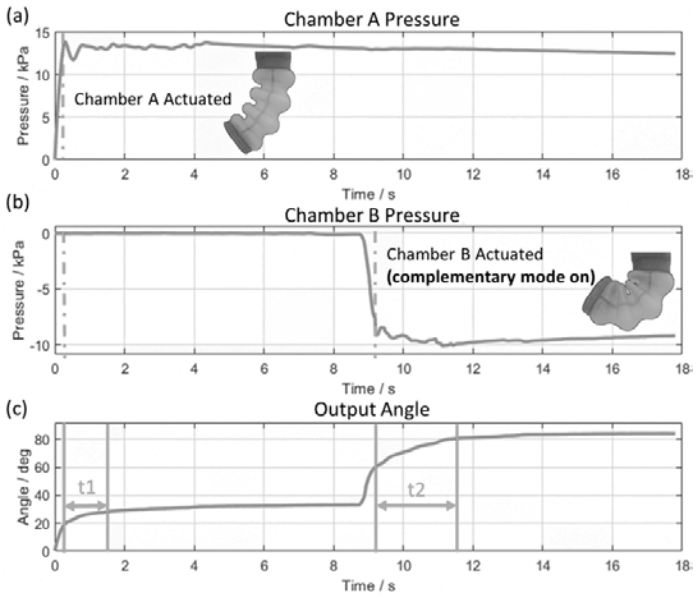

Fig. 7: Results of the two chamber pressure versus angle test. (a) Pressure in Chamber A. (b) Pressure in Chamber B. The rise times are calculated as: t1: 1.5 sec, t2: 1.9 sec. The pressure in Chamber A continues to drop over time as the volume is affected by the contraction in Chamber B. (c) Angle subtended by the actuator.

The maximum values of the actuators' input pressure, force, and angle are -25 to 22.3 kPa, 2.17 N, and 102.6°, respectively. The maximum pressure value was acquired by applying pressure until the actuator failed; the minimum pressure was determined by completely evacuating the actuator; the force and angle measurements were taken at slightly lower pressure values than the extremes (-24.5kPa and 22kPa) and measured in accordance with Fig. 3b and c.

5 Conclusion

This paper presents a multi-material 3D printed soft monolithic actuator that incorporates parallel symmetrical bellow chambers to implement bi-directional variable stiffness. Complementary and antagonistic control modes were proposed and implemented in the design while the two chambers can work collaboratively with either positive pressure or negative pressure. For pneumatic actuators that operate in the low-pressure region (< 20 kPa), output force and bending angle performance is always a challenge. Compared to actuators that can only be actuated in a single mode with either positive or negative pressure, the presented design achieves higher output force, larger bending angle, or tunable stiffness without the need to increase the driving pressure.

3D printing rather than silicone moulding introduces quicker prototyping, better reproducibility, and stronger interfacial bonds to the actuator. The test results confirm the high level of reproducibility with low deviation between test results. The actuator was fully physically characterised under two-chamber PI control. The results show that the proposed complementary and antagonistic control method is promising for future work in bi-directional bending actuators. The key metrics to take from the studies are: maximum angle of curvature 102.6°; maximum output force 2.17N; controlled force variability 1.56N; and maximum beam stiffness 0.96mN m^2. With the proposed complementary/antagonistic control modes, this design achieves a higher output force and comparable bending angles to the similar designs [6, 13] at a fraction of the driving pressure.

Future work plans to further explore the potential of this actuator design and investigate the possible applications in grasping and in-hand manipulation. The authors will investigate variations on this preliminary design: increasing the stiffness to improve force output; adding modularity; scaling down the size of the actuator; and adding tactile sensing as a means of feedback.

Supplementary video: `https://youtu.be/F-ANfUwE0XY`

References

1. Kim, S., Laschi, C., Trimmer, B.: Soft robotics: A bioinspired evolution in robotics (may 2013)
2. Abondance, S., Teeple, C.B., Wood, R.J.: A Dexterous Soft Robotic Hand for Delicate In-Hand Manipulation. IEEE Robotics and Automation Letters **5**(4), 5502–5509 (2020)
3. Iida, F., Laschi, C.: Soft robotics: Challenges and perspectives. In: Procedia Computer Science. vol. 7, pp. 99–102. Elsevier B.V. (jan 2011)
4. Manti, M., Cacucciolo, V., Cianchetti, M.: Stiffening in Soft Robotics: A Review of the State of the Art. IEEE Robotics & Automation Magazine **23**(3), 93–106 (sep 2016)
5. He, L., Leong, F., Dulantha Lalitharatne, T., de Lusignan, S., Nanayakkara, T.: A haptic mouse design with stiffening muscle layer for simulating guarding in abdominal palpation training. In: 2021 IEEE International Conference on Robotics and Automation (ICRA). IEEE (2021)

6. Babu, S.P.M., Sadeghi, A., Mondini, A., Mazzolai, B.: Antagonistic pneumatic actuators with variable stiffness for soft robotic applications. In: 2019 2nd IEEE International Conference on Soft Robotics (RoboSoft). pp. 283–288 (2019)
7. Suzumori, K., Wakimoto, S., Miyoshi, K., Iwata, K.: Long bending rubber mechanism combined contracting and extending fluidic actuators. In: IEEE International Conference on Intelligent Robots and Systems. pp. 4454–4459 (2013)
8. Chen, Y., Chung, H., Chen, B., Sun, Y.: A lobster-inspired bending module for compliant robotic applications. Bioinspir. Biomim **15**(5), 56009 (jul 2020)
9. Zhu, M., Mori, Y., Wakayama, T., Wada, A., Kawamura, S.: A Fully Multi-Material Three-Dimensional Printed Soft Gripper with Variable Stiffness for Robust Grasping. vol. 6, pp. 507–519 (2019)
10. Yirmibesoglu, O., Morrow, J., Walker, S.: Direct 3D printing of silicone elastomer soft robots and their performance comparison with molded counterparts. In: 2018 IEEE International Conference on Soft Robotics, RoboSoft 2018. pp. 295–302. Institute of Electrical and Electronics Engineers Inc. (jul 2018)
11. Sachyani Keneth, E., Kamyshny, A., Totaro, M., Beccai, L., Magdassi, S.: 3D Printing Materials for Soft Robotics. Advanced Materials (2020)
12. Yap, H.K., Ng, H.Y., Yeow, C.H.: High-Force Soft Printable Pneumatics for Soft Robotic Applications. Soft Robotics **3**(3), 144–158 (sep 2016)
13. Peele, B.N., Wallin, T.J., Zhao, H., Shepherd, R.F.: 3D printing antagonistic systems of artificial muscle using projection stereolithography. Bioinspiration and Biomimetics **10**(5), 055003 (sep 2015)
14. He, L., Tan, X., Suzumori, K., Nanayakkara, T.: A method to 3d print a programmable continuum actuator with single material using internal constraint. Sensors and Actuators A: Physical **324**, 112674 (2021)
15. Gul, J.Z., Sajid, M., Rehman, M.M., Siddiqui, G.U., Shah, I., Kim, K.H., Lee, J.W., Choi, K.H.: 3D printing for soft robotics–a review (dec 2018)
16. Zolfagharian, A., Mahmud, M.A., Gharaie, S., Bodaghi, M., Kouzani, A.Z., Kaynak, A.: 3D/4D-printed bending-type soft pneumatic actuators: fabrication, modelling, and control. Virtual and Physical Prototyping **15**(4), 373–402 (2020)
17. Smooth-On: Ecoflex 00-30 product information, `https://www.smooth-on.com/products/ecoflex-00-30/`
18. Stratasys: Agilus 30, `https://www.stratasys.com/materials/search/agilus30`
19. Dammer, G., Gablenz, S., Hildebrandt, A., Major, Z.: Design and shape optimization of PolyJet bellows actuators. In: 2018 IEEE International Conference on Soft Robotics (RoboSoft). pp. 282–287. IEEE (apr 2018)